RESEARCH ARTICLE

Use of covalent dynamic networks as binders on epoxy-based carbon fiber composites: Effect on properties, processing, and recyclability

Julio Vidal[1] | Carlos Hornero[2] | Ruth Garcia[3] | Jesus Cuartero[4] |
Anne Beaucamp[5] | Maurice N. Collins[5,6] | Lidia Garcia[7] |
David Ponce[1] | Mari Carme Royo[3] | Elisabeth Sanchez[3] | Pere Castell[1,8]

[1]Fundación Aitiip, Zaragoza, Spain

[2]Moses Productos S.L., Zaragoza, Spain

[3]Leitat Technological Center, Terrassa, Spain

[4]Department of Mechanical Engineering, University of Zaragoza, Zaragoza, Spain

[5]School of Engineering, Bernal Institute, University of Limerick, Limerick, Ireland

[6]AMBER, University of Limerick, Limerick, Ireland

[7]Tecnopackaging, Zaragoza, Spain

[8]GCR Group, La Bisbal del Penedès, Spain

Correspondence
Julio Vidal, Fundación Aitiip, Pol. Ind. Empresarium C/Romero, 12, 50720 Zaragoza, Spain.
Email: julio.vidal@aitiip.com

Abstract

Composites are gaining widespread market interest due to their outstanding mechanical properties and light weight. However, this growth is hindered by the lack of sustainable recycling solutions. This research aims to integrate reversible chemistries to advanced carbon fiber-reinforced composite materials for recycling in a so-called eco-design, circular approach. Diene and dienophile reactions are generated at the surface of the carbon fiber allowing a bond–debond interaction with the epoxy matrix. The application of the Diels–Alder adduct on the fiber modifies its polarity and structure. This research assesses a biobased and synthetic epoxy equivalent and demonstrates that this newly developed interphase chemistry has a direct impact on the crosslinking efficiency of the resin, as well as on their interlaminar properties. Furthermore, it has been observed that depending on the type of resin, these changes can have differing impacts on final properties of the composite, reducing the crosslinking density up to 50% in some modifications while in others the T_g remains constant.

KEYWORDS
carbon fiber, composites, Diels–Alder, eco-design, fiber treatments

1 | INTRODUCTION

Composite materials are widely used in many sectors, such as automotive,[1] construction,[2] energy,[3] railway,[4] aeronautics,[5] aerospace,[6] and so forth and they can be classified according to thermostability of the matrix used: thermoplastic,[7,8] elastomer,[9] and thermoset.[10] The focus in the present study is set on thermoset composite materials due to their outstanding mechanical performance while reducing weight and eliminating corrosion or degradation concerns. However, processing is more expensive in comparison to the other composite classes. For thermoplastic[11] and elastomers, it is possible to melt the material, and this allows recyling within more cost effective processes.[12] On the other hand, thermosets cannot be reprocessed/recycled by means of conventional procedures. In the current

context of increasing climate awareness and the growing concerns around efficient usage of resources while decreasing and ultimately achieving net zero carbon emissions. The ability to recycle high-performance thermoset materials has come sharply into focus as these materials will be deployed in electric vehicles and wind turbine blades as well as other critical infrastructure for the emerging circular economy where end of life scenarios dictate overall life cycle analysis.[13] Carbon-fiber-is one of the most used fibers to reinforce matrices to improve the mechanical performance of the final material.[14] Carbon fiber-reinforced polymers (CFRP) are widely used in structures and industries as a substitute for metals.[15–17] In this study, we focus on continuous woven carbon fiber as a reinforcement. This woven structure is ideal for applications where high strength-to-weight and high stiffness-to-weight ratios are of importance: aerospace, automotive, sporting goods, wind turbines, or railway.[18] CFRP demand is expected to grow rapidly with the boom of electric vehicles (EVs).[19] Although CFRPs in general are well developed and studied, there are still many unknowns and this has been acerbated by the emergence of bioresins/matrices and how they interact with differing fibers and their weaves in dynamic environments.[20,21]

The third component of a composite is the binder,[22] which is less studied as it is not always necessary, its chemistry depends on the chemistry of both matrix and reinforcement.[23] The binder improves the final properties of the composite material and can be derived from fossil based or bio-based resources.[24] It is often used to improve the interface between the matrix and the fiber.[25] In the case of carbon fiber, some of the most used binders are molecules with polar groups[26] such as silanes, as the CF does not contain these groups,[27] with the overall intention of avoiding failure at the interphase.[28,29]

In order to fully incorporate thermoset composites into a circular economy system or to implement eco-design, the binder must be addressed as the binders as well as the crosslinks hold the system together and renders recycling impossible. In this context, the work developed and described within this manuscript is focused on the development of a binder that is capable of bonding the matrix and fibers together but also allows their separation by the application of an external stimulus. Bringing thermoset composites, a step closer to the circular economy and recylability.

Although in this research, the focus has been placed on the binder and its capacity to link together fiber and resin. It is important to consider all the components and research that surrounds the carbon fiber thermoset composites which are aiding the transition of CFRP toward the circular economy,[30] such as the development of bio-based carbon fiber,[31,32] development of biobased epoxy resins.[33] And, research based on the optimization of recycling strategies: pyrolysis[34] and solvolysis.[35] The issue in all these cases in the inability to separate and treat properly the different components of the composite.

Covalent dynamic networks (CDNs) have the capacity to cleave bonds upon exposure to external stimuli, such as light or heat.[12,36,37] The ability to cleave and reverse a covalent bond renders them of great interest to composite materials offering the possibility of a new generation of recyclable thermosetting structures.[38–40]

The chemical mechanism depends on the nature of the molecule used, and its capacity to generate and cleave bonds. Here, we focus on the Diels–Alder (D–A) mechanism, which is categorized as dissociative. It involves the generation of a cyclohexene by an equilibrium reaction of a diene and a dienophile while the equilibrium can be shifted toward the formation of the cycle or backwards to the presence of both diene and dienophile. Due to this equilibrium and the possibility of controlling it on demand that the D–A mechanism can be used as a strategy for the generation of CDN.[41] In the study, we focus on biobased structures to produce the CDN. The nature of the epoxy groups is quite unstable and it is targeted for cleavage between the two carbons and the oxygen. Usually, a nucleophile such as nitrogen present in amines is used to provide electrons to the system and allow the epoxy ring to open generating a 3D structure. To incorporate the chosen D–A structure into the epoxy resin system the structure developed by Susana et al[42] was modified by substituting the OH group with a NH group. This allows the epoxy resin to react with the D–A adduct in similar way to standard epoxy curing.

Through the selection of the adduct, it has been possible to treat the CF surface with the D–A structure. This has allowed to study the effect and potential that the application of a CDN structure in the surface of the fiber have in the composite.[43] As well as how its application in the composites should be targeted to enable the separation of both matrix and reinforcement bringing the composite industry a step closer to the circular goals.[44]

The present study opens a new path for the recycling process as it facilitates the separation of fibers and matrices through the application of an external stimuli to the D–A that chemically separates both the carbon fiber and the epoxy resin. To achieve this goal, this study has worked on different methodologies that enable anchoring and formation of the D–A adduct on the surface of the CF while monitoring changes in the fiber after each treatment. Composites are manufactured from the treated fibers using a biobased and a synthetic resin and characterized thermally, mechanically and spectroscopically. ΔH is calculated for each system to determine the energy provided to the polymeric chains of the matrix to allow them to flow/move.

Overall, the present study produces a methodology to generate D–A adducts on the surface of carbon fibers and studies the impact of this reversible system on the interphase of the carbon fiber of typical thermoset matrices and how these interfacial interactions impact overall composite performance while bringing thermoset composites a step closer to sustainability.

2 | MATERIALS AND METHODS

2.1 | Materials

The carbon fiber fabric (6K filaments, satin weave, 390 g/m^2) was kindly supplied by IDEC (Alava, Spain). The chemical materials used to treat the fibers tetraethylenepentamine (TEPA), 1,1′-(Methylenedi-4,1.phenylene)bismaleimide (BMI) and furfurylamine (FA) were acquired from MERCK (Amsterdam, Netherlands). The solvents: DMF and chloroform were purchased from Gilca S.A. (Zaragoza, Spain). Two different commercial epoxy resins have been used during the study for the formation of the final composite materials: Infugreen with the 4770-hardener purchased to MEL composites (Barcelona, Spain), the infugreen resin is a partially biobased resin that is commercially available, developed by sicomin and marketed as greenpoxy. With a biobased content ranging from 52% to a minimum of 22%. In the case of the infugreen resin system, the percentage of biobased carbon content is 29%, although in the epoxy resin alone it goes up to a 38% of plant-based carbon.

Although the second epoxy resin was a synthetic Hexion Epikote rimr035C with the Epikure RIMH037 as hardener. It was purchased from Hexion (Columbus, Ohio, EEUU), which is based mainly on Bisphenol-A and widely used in sporting goods and wind turbines.

Consumables used in the composite preparation were provided by MEL.

2.2 | Chemical synthesis of the D–A adducts and adduct application

The CF fabric was treated using a Tetra-30-LF-PC (Diener Electronic GmbH) plasma equipment, based on a vacuum chamber of 34 L with four trays symmetrically placed between five plane electrodes connected by a low-frequency generator (40 kHz and 1.0 kW). Two methodologies were used:

- Method 1: Consists of the plasma-enhanced chemical vapor deposition (PECVD) of acetic acid onto the carbon fiber, for the generation of different alcohol and carboxylic groups at the surface of the CF. This methodology consists of a two-step process, beginning with a surface activation (16sccm He and 16sccm air, 900 W, 30 min) followed by the PECVD of acetic acid (20sccm He as carrier gas, 900 W, 30 min). The treated samples were stored in aluminum sealed bags under vacuum. Afterwards, the TEPA was incorporated onto the fiber by inserting the fibers into a TEPA bath, for 17 h at 190°C.
- Method 2: In this case, the fibers are directly treated with N$_2$ plasma, to incorporate aminated groups onto the fiber surface instead of oxygen groups. To achieve this goal, the plasma amination takes place under a mixture of 16sccm N$_2$ and 16sccm He plasma, at 900 W for 30 min. After the generation of the amino groups at the surface of the CF, it is sealed under vacuum conditions in an aluminum bag.

Afterwards, fibers are treated with a saturated solution of BMI in DMF.[45] CFs are sprayed with the BMI solution and dried at 80°C for 2 h. Then fibers are washed with DMF and acetone to remove unreacted BMI and fibers are then sprayed, with FA (3.84 M) in chloroform, and dried at 55°C for 21 h. Finally, the fibers are washed again with chloroform to remove unreacted FA.

2.3 | Characterization of the textile

Water contact angle (WCA) measurements were carried out with a Krüss K100 MK2 Tensiometer (Germany), applying Wilhelmy method. CF fabric were cut to 20×20 mm samples, attached to the sample holder and placed perpendicular to the test liquid. The wetted length of the samples was measured at room temperature with n-hexane as test liquid. The procedure consisted of measuring the force acting in the tensile direction when moving the CF fabric vertically in n-hexane at a constant speed. The detection sensitivity was set to 0.005 g, the measuring speed at 3 mm/min, and the maximum immersion depth at 5 ± 0.2 mm. Each sample was tested at least five times in different areas, and the mean wetted length was calculated using the Wilhelmy equation:

$$\gamma_{L/V} = F_{w} \cdot L_{w} \cdot \cos \theta \quad (1)$$

where $\gamma_{L/V}$ is n-hexane surface tension (18.4 mN/m), F_w is the measured force in N, L_w is the wetted length and θ is the contact angle with n-hexane, that is 0°.

The WCA of the fibers was measured by using deionized water as a test liquid. Measurements were carried out at room temperature, with a detection sensitivity set

to 0.005 g, a measuring speed of 10 mm/min and a maximum immersion depth of 3 ± 0.2 mm. Each fiber was dipped in and withdrawn from the liquid vessel at a constant velocity, to measure respectively the dynamic advancing and receding contact angles. Each sample was tested at least five times in different areas, and the mean contact angle was calculated using Wilhelmy equation.

A Renishaw (Barelona, Spain) in Via-reflex model spectrometer was utilized to analyze the Raman signatures of the CF. The measurement was operated in a continuous scanning mode at room temperature, and a green 514-nm argon ion laser was employed as the incident radiation. The laser beam was polarized parallel to the fiber axis and focused to give a spot size of 2-μm diameter on the fiber surface. The typical exposure time for all the samples was set to 60 seconds.

The graphite particle size La was determined using the Tuinstra and Koenig equation (Tuinstra and Koenig 1970) as follow:

$$L_a = C(\lambda)\left(\frac{I_D}{I_G}\right)^{-1} \qquad (2)$$

With $C(\lambda) = 4.4$ nm for a 514 nm laser radiation and I_D and I_G the height of the deconvoluted Raman bands using four modes D^* (1050–1200 cm^{-1}), D (1350–1370 cm^{-1}), D'' (1500–1550 cm^{-1}), and G (1580–1610 cm^{-1}).[46]

The capability of the D–A adducts to cleave and regenerate the bond on the treated CFs was tested using differential scanning calorimetry (DSC) as described by Susana et al.[41] A METTER TOLEDO DSC 3+ Star System (Columbus, Ohio, EEUU) was used. The cycles applied to the samples consisted of heating from room temperature to 120°C at 5°C/min, and measuring the change in the energy absorption. After the sample was heated inside the DSC equipment, it was left for 21 h at 60°C in the oven to enable the D–A to regenerate. This two-step process, with the control cleave of the D–A adduct and posterior regeneration of the bond compose one cycle of the study. During the whole process, the fibers cut from the treated textile and placed into the DSC capsule are not removed from it, and the capsule is kept closed.

2.4 | Liquid resin infusion for composite production

Manufacturing of composite parts is carried out via liquid resin infusion (LRI). Table 1 shows the thermal treatments used in the preparation of each of the composites, as well as the dimensions and number of specimens obtained. Each composites consists of three layers of treated CF with the D–A adduct. Each of the layers has a thickness of 0.7 mm, and despite a gain in stiffness after the treatments all fibers adapt easily and without breaking, to the flat shape provided by the vacuum bag.

To ensure that all composites are processed under the same conditions, the infusion of treated and untreated fibers is done simultaneously as shown in Figure 1.

2.4.1 | Characterization techniques used on the composite

Thermomechanical properties of the CFRP were analyzed using a dynamic mechanical analysis (DMA) Q800 (TA, Austin, USA). Samples of $17.5 \times 12 \times 40$ mm^3 were tested in single cantilever mode in a temperature ramp
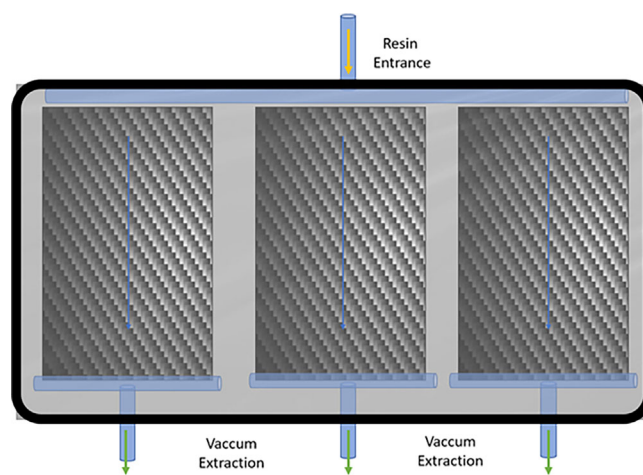
FIGURE 1 Representation of the liquid resin infusion manufacturing process carried out with each of the composite resins.

TABLE 1 Data on the thermal treatment applied for the LRI processing of composites with each of the selected resins as well as the thickness and number of specimens obtained for the DMA and interlaminar shear strength.

Resin name	Thickness (mm)	Curing process	Post-curing process	DMA		Interlaminar	
				No D–A	With D–A	No D–A	With D–A
Epikote	1.4	3 h at 80°C	1 h at 120°C	5	10	7	50
Infugreen	2	3 h at 80°C	1 h at 120°C	5	10	10	50

Abbreviations: LRI, liquid resin infusion; DMA, dynamic mechanical analysis.

from -100 to $150°C$ with a ramp of $1°C/min$, $10\ \mu m$ amplitude and several frequencies (1, 5, 10, and 50 Hz).

For the linear viscoelastic materials, the complex modulus E^* is the expression of the storage modulus E' and the loss modulus E'' such as:

$$E^* = E' + E'' \tag{3}$$

The ratio of the moduli is defined as the damping Tan δ such as:

$$\mathrm{Tan}\,\delta = \frac{E''}{E'} \tag{4}$$

The temperature range of the glass transition is measured between the temperature of the inflection point of the curve of storage modulus and the temperature of the peak of the tan delta, according to the ISO 6721-11 standard. T_g is measured at the peak of the loss modulus.

The activation energy (ΔH) is derived from the Arrhenius law as described by Li et al.[47] Briefly, ΔH is determined by superimposition of the tan δ peaks at different test frequencies. The temperature dependence of the test frequency is expressed by

$$f = f_0 \exp\left(-\frac{\Delta H}{RT}\right) \tag{5}$$

where f and f_o are analogous to the rate constant and pre-exponential factor of the Arrhenius equation and R is the gas constant.

For two glass transition temperatures, T_{g1} and T_{g2} at frequencies respectively f_1 and f_2, the ratio of f_1 and f_2 is:

$$\frac{f_1}{f_2} = \frac{\exp\left(-\frac{\Delta H}{R}\left(\frac{1}{T_{g1}}\right)\right)}{\exp\left(-\frac{\Delta H}{R}\left(\frac{1}{T_{g2}}\right)\right)} \tag{6}$$

$$\ln\left(\frac{f_1}{f_2}\right) = \frac{\Delta H}{R}\left(\frac{1}{T_{g2}} - \frac{1}{T_{g1}}\right) \tag{7}$$

For a small increment between T_{g1} and T_{g2},

$$\Delta H = -R \cdot \left[\frac{d(\ln(f))}{d\left(\frac{1}{T_g}\right)}\right] \tag{8}$$

where ΔH is the activation enthalpy of the glass transition relaxation; R which is the Arrhenius constant; f which is the frequency of the experiment; and T_g which is the glass transition temperature.

Therefore, it has been possible to calculate the T_g of each of the composites manufactured at all different frequencies tested ΔH was derived from the slope of the plot of ln (f) versus $1/T_g$. In the case of the composites, the E_a implies the energy that it is necessary to provide to the material to start observing movement and displacement of the different polymeric chains among each other.

For the interlaminar tests, a hydraulic Instron 8032 with a load cell of 5 kN was used. The sample preparation needed in order to follow the ISO 14130, determination of apparent interlamellar shear strength by short-beam method, was to cut samples of $10 \times 20\ mm^2$. These samples along with samples used for the DMA were prepared by water-jet cutting with all yarns orientated at $0°$ or $90°$.

For the SEM study, the equipment used was a SEM Hitachi 3400N available in the ICB-CSIC (Zaragoza, Spain). It can be used with different electron acceleration voltages, emitting in a range from 1 to 30 kV. In this case, the sample fractographs were analyzed without any pretreatment.

3 | RESULTS AND DISCUSSION

Contact angle measurements allows changes in polarity of the CF to be assessed thereby enabling the comparison of both fiber treatments (Figures 2 and 3), through the application of the Formula 1.

The incorporation of new amino groups at the surface of the fiber infers a reduction in the contact angle implying increased hydrophilicity, for the TEPA this reduction is quite small, as shown in Figure 4, and this is attributed to its long hydrophobic carbon chain. The incorporation of the BMI, which is a highly non-polar molecule, increases the hydrophobicity and those present in the TEPA, reducing the polarity and enabling a better interaction between the fiber and the solvent used (n-hexane). Finally, as the FA is incorporated the contact angle drops, due to the presence of the amine group, which will be used as anchor with the epoxy group and increases again the polarity of the sample reducing the compatibility between fiber and solvent.

These results were confirmed using deionized water. In this case, the behavior of both methods in the first step is sharply differentiated, while adding the TEPA the wettability is decreased as an effect of the non-polar carbon chains, the amino groups generated by plasma on the surface of the fiber do not alter significantly its wettability.

Nevertheless, the incorporation of the BMI molecule drops the wettability of all samples to 5 mm, which is completely aligned with the effect observed in the contact angle and with the nature of the BMI molecule, in which there is no polar group and the therefore interaction with a liquid such as water is not favored. Finally, in the
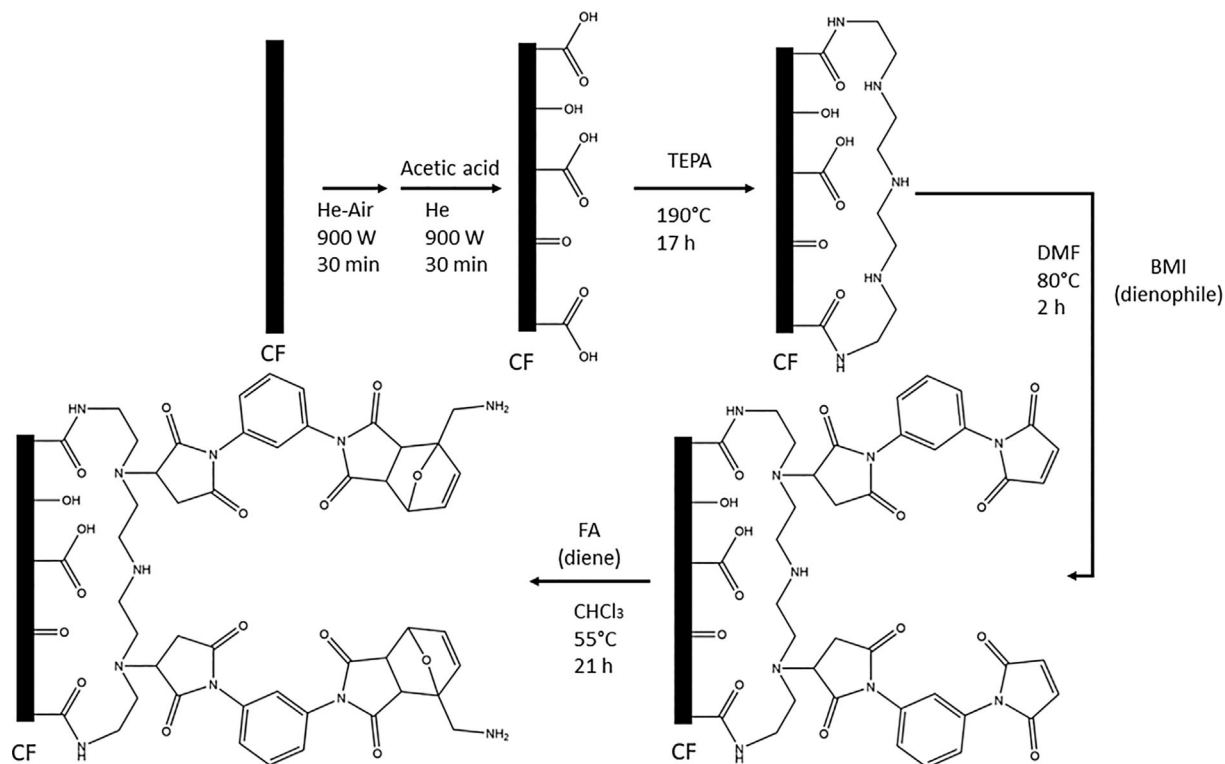
FIGURE 2 Scheme of the first method to incorporate the D–A structure into the surface of the CF.
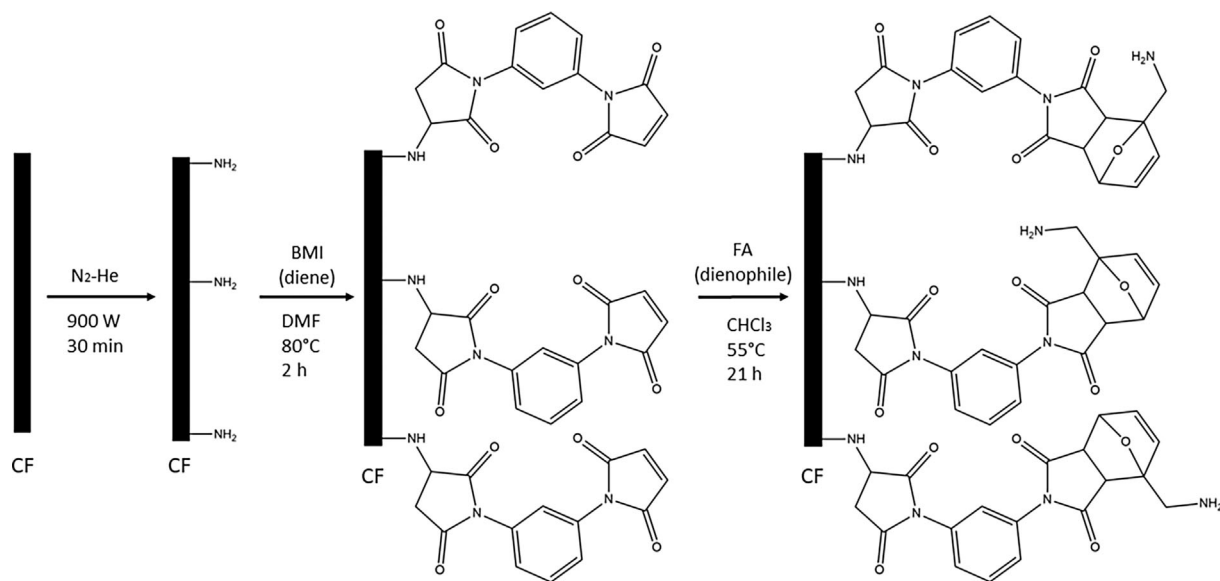

FIGURE 3 Scheme of the second method to incorporate the D–A structure into the surface of the CF.

incorporation of the FA, by reacting with the BMI, generates an increment in the wettability, which can be again associated with the polarity of the molecule and the amine group in the external part of the fiber, see Figure 5. Nevertheless, this effect, it is not observed in the first methodology (Using TEPA), which implies that the reaction between the BMI anchored to the amine groups of the TEPA and the FA might not be taking place possibly due to stereochemical hinderances.

It was decided then to follow the study with the second proposed methodology, as with the TEPA results were not very promising, although in all steps of the fiber treatment it was possible to see appearance changes (yellowish color, stiffness).
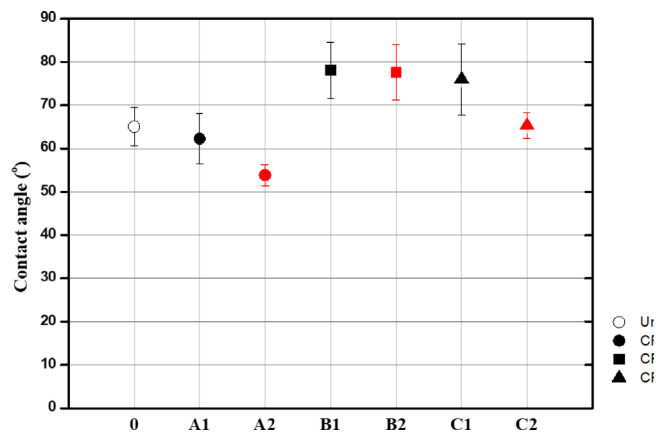
FIGURE 4 Contact angle of the carbon fiber textiles before and after each of the surface treatments (0: Untreated CF; A1: CF treated with TEPA; A2: CF aminated; B1: CF treated with TEPA+BMI; B2: CF aminated and treated with BMI; C1: CF treated with TEPA+BMI + FA; C2: CF aminated and treated with BMI + FA).

FIGURE 5 Wettability of the carbon fiber textiles before and after each of the surface treatments (0: Untreated CF; A1: CF treated with TEPA; A2: CF aminated; B1: CF treated with TEPA+BMI; B2: CF aminated and treated with BMI; C1: CF treated with TEPA+BMI + FA; C2: CF aminated and treated with BMI+FA).
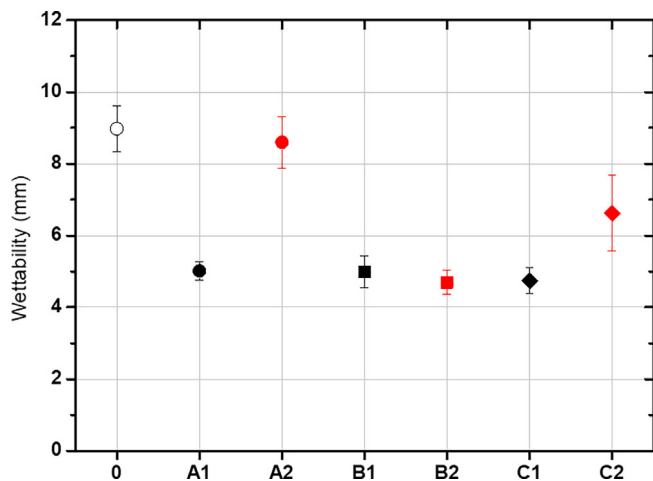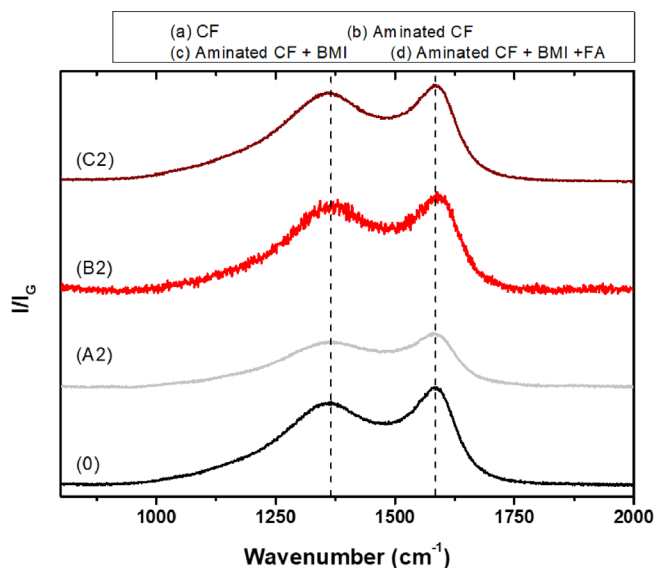

FIGURE 6 Raman specters obtained at 514 nm wavelength for the CF before and after the treatments (0: Untreated CF; A2: CF aminated; B2: CF aminated and treated with BMI; C2: CF aminated and treated with BMI+FA).
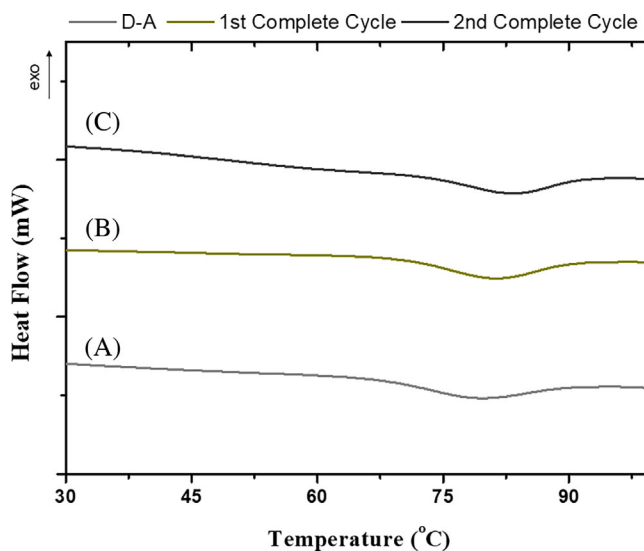
FIGURE 7 DSC thermograms on the treated CF; (A) treated CF; (B) treated carbon fiber after one heating cycle; (C) treated carbon fiber after two heating cycle.

The effect of the D–A treatment through amination on the quality of the carbon phase was assessed using Raman spectroscopy on the carbon bands. All the plots present two peaks centered respectively at 1360 and 1592 cm^{-1} (Figure S1; Calculation of the I_D and I_G of the Raman spectroscopy over the different samples CF sample), due respectively to the defects (D band) and to the ordered graphitic carbon (G band). The results are plotted in Figure 6 and tabulated in Table S2. The treated fibers present Raman spectra with a D band that remains centered at 1360 cm^{-1} and a G band that shifts toward higher wavenumber. This shift is accredited to the intercalation of dopants during the functionalization of CFs. Furthermore, the increase of the I_D/I_G ratio as the functionalization is furthered is due to the increase in defect density in the CFs.[41]

With the diene and the dienophile incorporated into the fibers structure, three different heating cycles, taking the material from room temperature to 120°C and afterwards leaving it at 60°C for 21 h, were applied in order to corroborate the presence of the cyclohexene and the reversibility of the bond. As observed in Figure 7, the first

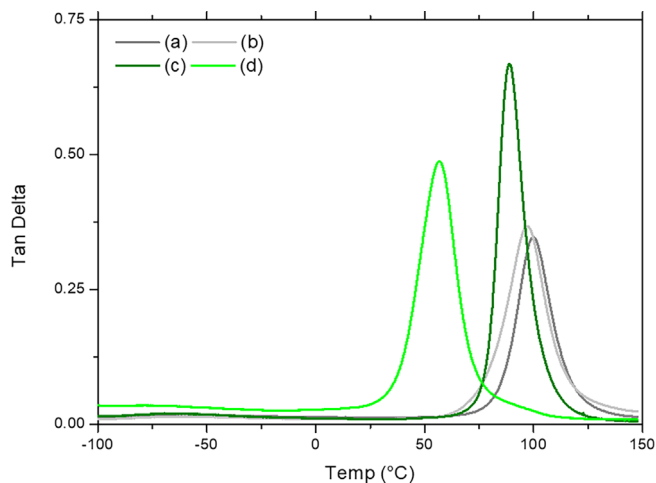**FIGURE 8** Loss modulus and Tan Delta of the composites measured at 1 Hz (A: Epikote resin with untreated CF; B: epikote resin with treated CF; C: Infugreen resin with untreated CF; D: Infugreen resin with treated CF).
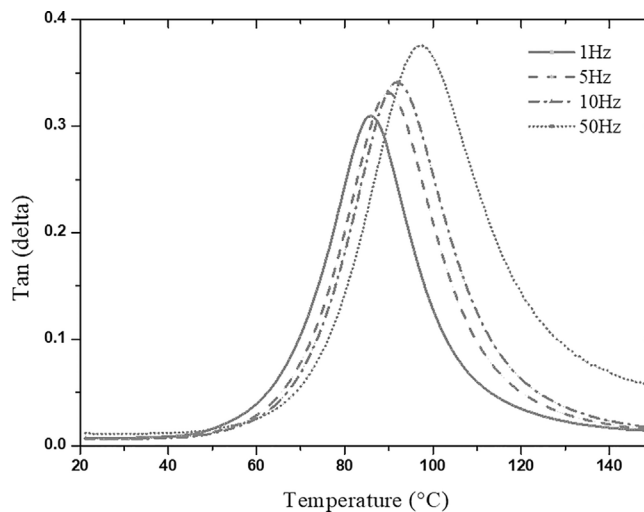

FIGURE 9 Representation of the Tan Delta at four different frequencies (1 Hz; 5 Hz; 10 Hz; 50 Hz) for the biobased epikote epoxy resin with treated CF.

time the treated CF is exposed to the heating process there is an endothermic process taking place at around 80°C related with the cleave of the cyclohexene into diene and dienophile, and this is supported by literature.[37] After thermal treatment at 60°C, the cleavage reaction occurs again upon the second heating cycle. This was performed three times, demonstrating that the adduct can be cleaved and regenerated and shows the potential for ease of separation of CF from the matrix, thereby allowing recycling, aligning the results obtained to those observed in the literature.[37]

These DSC studies demonstrated the presence of the D–A adduct on the surface of the fiber and the capacity of displacing the D–A equilibrium toward the diene and dienophile at high temperatures to recover the cyclohexene after the exposure to a mild temperature.

As shown in Figure 8, the DMA analysis the impact of the D–A adducts on crosslinking, and therefore on the T_g, is clearly evident especially for the biobased epoxy. For synthetic Epikote resin, the presence of the adducts reduces the T_g by 9°C (from 83.7 to 74.7°C), however, the adduct treatment on the fiber has little overall influence on the viscoelastic behavior (high elasticity and low damping behavior) of the synthetic resin, whereas for the biobased infugreen resin the effect that the presence of the D–A adducts on the T_g is more stark with a ~40°C reduction (from 76.7 to 35.9°C). The treatment has little influence on elasticity while the damping behavior is reduced due to the presence of the D–A adducts.

In Figure 9, the epikote synthetic epoxy resin, is assessed in terms of the influence of the D–A adducts on T_g, damping, activation energy (E_a) and elastic modulus (E'),[42,48] such calculation was possible by the application

of the formulas (III–VIII) described in the materials and method chapter. As described above the T_g, is reduced and this is attributed to interference with crosslinking as there is competition for reactive sites between the adduct and the crosslinking agent (hardener), thereby reducing crosslinking densities when compared to untreated equivalent samples.

For the biobased Infugreen epoxy resin, all parameters (T_g, E_a and E') are influenced by the D–A adduct treatment. Crosslinking densities are lowered with the knock-on effect of a greatly reduced T_g and E'.[43] With mobility of the polymeric chains reduced by around 30%, the damping values reduce accordingly from 0.66 to 0.48, resulting in an increase in ductility by more than 20% as observed from values calculated for the E_a, see Table 2.[49]

As it is observed by looking at the reduction in the T_g, the presence of the D–A adduct on the surface of the carbon fibers impacts the crosslinking of the infugreen biobased epoxy resin more than the synthetic epikote. These changes in the T_g and its implications with the crosslinking imply that the nature of the amino group introduced into the fibers generates a competitive reaction with the epoxy groups.

In the case of the synthetic epitoke resin, the competition of the amino groups is not very exacerbated as the crosslinking of the resin is barely affected by their presence. Whereas, in the case of the biobased infugreen resin, the competition is higher generating a substantial drop in the crosslinking and therefore in the T_g, as an effect of the reaction that takes place between the D–A adduct and the epoxy groups. From the results, it is obvious that the bonding between the adducts anchored to the CF and the epoxy resin is faster than the crosslinking

TABLE 2 Values obtained in the dynamic mechanical analysis measurements and posterior calculations with each of the composites.

Sample	T_g (°C) range (3°C/min, 1 Hz)	Max damping	E_a (kJ mol^{-1})	E' (rubbery plateau) (MPa)
Untreated fiber synthetic epikote resin	83.7–99.9	0.34	352.8 ± 18.9	2963
Treated fiber synthetic epikote resin	74.7–97.0	0.36	384.1 ± 15.0	2294
Untreated fiber biobased infugreen resin	76.1–88.5	0.66	331.0 ± 13.5	1060
Treated fiber biobased infugreen resin	35.8–56.7	0.48	261.6 ± 0.7	815

of the epoxy resin affecting significantly the properties of the matrix.

Once, it was observed that the presence of the adduct have a direct impact in the crosslinking and properties of the resins, it was proposed to carry out and measure the change in the delamination in order to understand how the adduct was affecting the interlaminar properties. In Table S3, it is possible to observe that for the epikote resin a 10 MPa difference is observed, while for the infugreen resin the difference is up to 30 MPa reduction from the untreated the treated sample (49.4–17.0 MPa).

Thermal treatment has little effect on the syntetic resin with delamination values in the same range around a 30% lower than without the thermal treatment. This is directly related with the results observed in the DMA. The resin is fully cured and additional thermal treatments are not required. Therefore, it is possible to conclude that the presence of the D–A adducts at the surface of the fiber reduces the T_g and the interlaminar properties of this resin. Although the adduct is formed and broken by the application of temperature, as shown in Figure 7, its effect is not critical as a drop in the interlaminar forces is not observed when going over the equilibrium temperature and the clevage of the D–A adducts is taking place.

In the case of the infugreen resin, the thermal treatments have a major influence on the interlaminar properties of the composites. Values obtained in these cases show an increment of more than 100% depending on the final thermal treatment applied. There is a clear trend between the interlaminar forces and post-thermal treatment, as the temperature and time of the post-treatment increases, the interlaminar forces increase. This shows a direct relation between the temperature of the post treatment and the interlaminar properties, which implies that the energy provided by the post-treatment improves the bonding between the fiber and the biobased resin matrix which is preventing to see any effect coming from the adduct.

In this regard, further study is needed in order to fully understand and determine the optimal thermal treatment for the biobased resin and to determine how it interacts during the curing process with the adducts applied to the
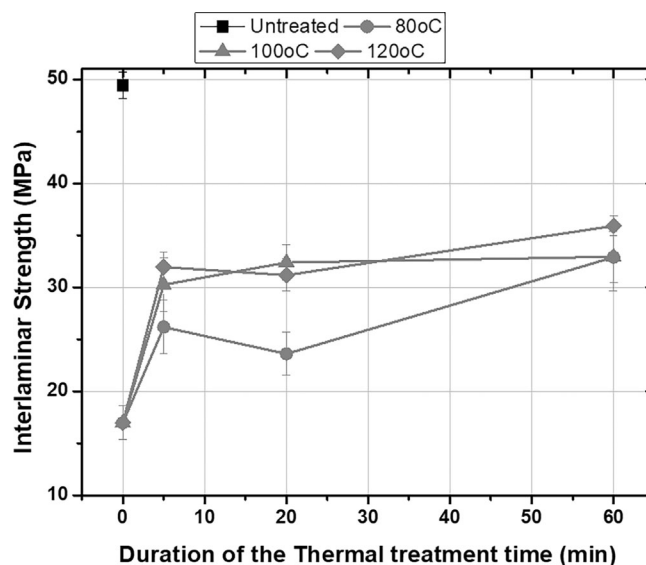

FIGURE 10 Effect of thermal treatments on the interlaminar strength of the infugreen composites (A: Infugreen resin with untreated CF; B: Infugreen resin with treated CF and a thermal post-treatment at 80°C; C: Infugreen resin with treated CF and a thermal post-treatment at 100°C; D: Infugreen resin with treated CF and a thermal post-treatment at 120°C).

fibers surface. As observable in Table S3 and Figure 10, a rapid increase in the delamination strength is observed with treatments at 100 and 120°C, maintaining similar ranges of strength after 5 min of treatment. Whereas in the case of the 80°C thermal treatment, the increase is gradual reaching 30 MPa after 60 min of treatment. For the synthetic epikote resin, all strengths measured are in the same range not being improved.

This improvement of the interlaminar strength with temperature for the biobased infugreen is related to the amount of epoxy resin polymeric chains that remain uncrosslinked and are therefore available to react with the amino group incorporated in the fiber with the D–A group. This correlates directly with data obtained in the DMA that shows a lower T_g for the infugreen treated samples.

Finally, in the SEM micrographs shown in Figure 11, a clear difference in the interaction between the treated

and the untreated samples is observed. For treated samples, a clearly differentiated gap is observable between the fiber and the resin. This implies that the interaction between the fiber and matrix is being negatively influenced by the presence of the D–A adduct at the interfacial region.

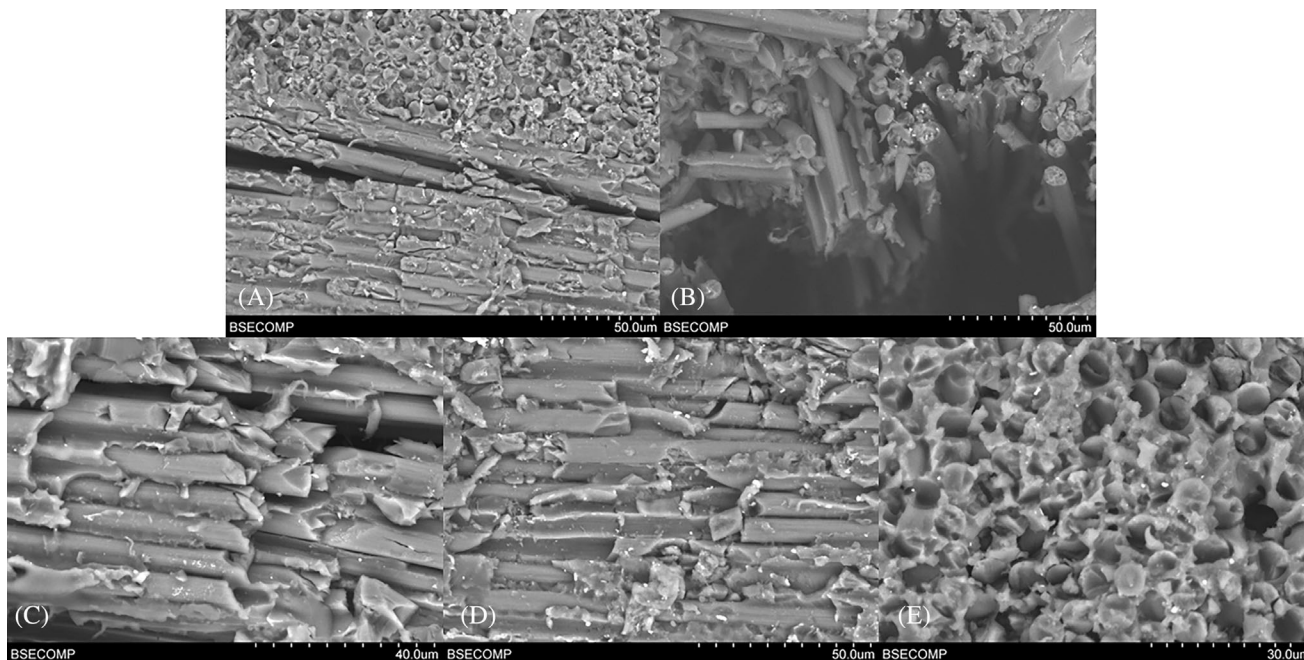Micrographs of both epikote (Figure 11) and infugreen (Figure 12) resin show the same characteristics, a

FIGURE 11 (A) Epikote without D–A (×650); (B) Epikote with D–A (×800); (C) Epikote with D–A and a thermal treatment of 60 min at 100°C (×1300); (D) Epikote with D–A and a thermal treatment of 60 min at 100°C (×1000); (E) Epikote with D–A and a thermal treatment of 60 min at 120°C (×1500).

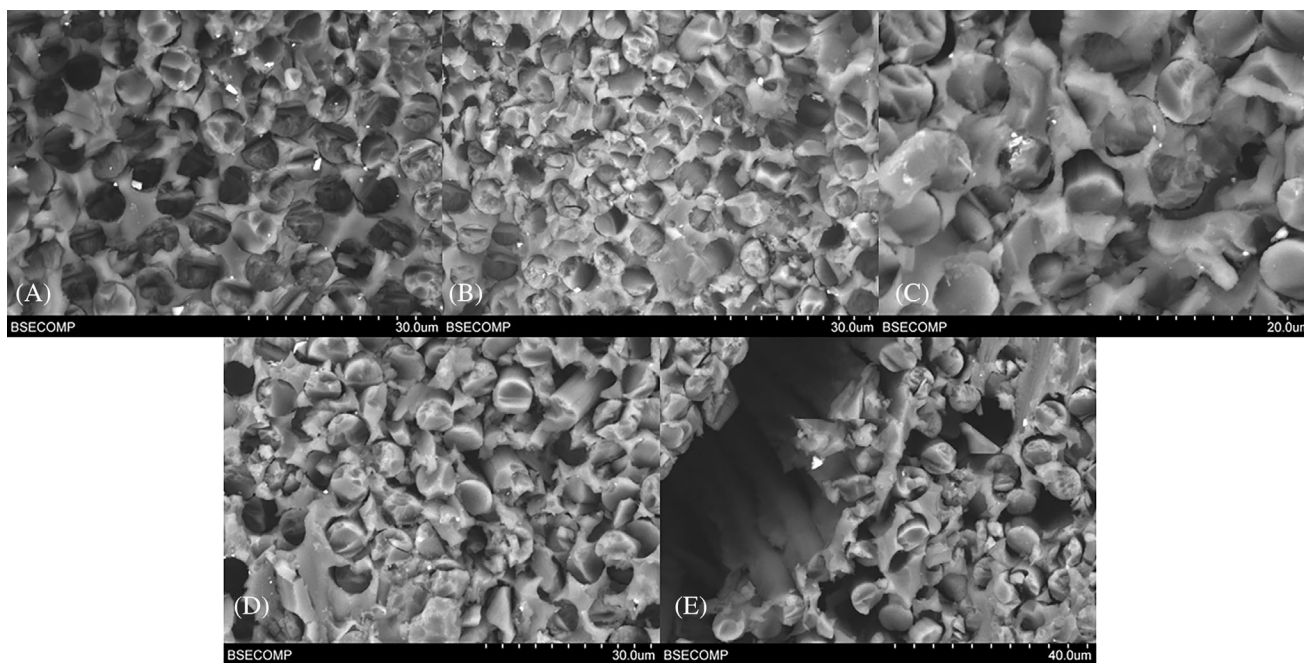**FIGURE 12** (A) Infugreen without D–A (×1800); (B) infugreen with D–A (×1500); (C) infugreen with D–A and a thermal treatment of 60 min at 100°C (×2700); (D) infugreen with D–A and a thermal treatment of 60 min at 100°C (×1600); (E) infugreen with D–A and a thermal treatment of 60 min at 120°C (×1400).

fiber that comes in direct contact with the matrix and each matrix surrounds the fiber during the infusion.

Post-thermal treatments shows how the interaction between fiber and matrix improves without reaching the same homogeneity observed in the case of the untreated fibers for the case of the composites manufactured with the infugreen resin. Whereas in the case of the epikote resin, it is not possible to perceive any difference among the thermal treated samples.

4 | CONCLUSIONS

The application of a D–A adducts and reaction mechanisms in composites to enable the separation of the components is a new concept that will adapt composites toward a more sustainable and circular economy, through the implementation of new binders. A cyclohexene is generated at the surface of the carbon and is in equilibrium state with the diene and dienophile forms. This allows bonding-debonding capacity of this newly developed reversible binder.

In this research, the capacity to synthesize and anchor the adduct directly onto the surface of carbon fibers has been demonstrated and the changes to the properties of the fibers have been monitored, as a function of structure/property/processing relationships of the final composite material.

The presence of the adducts at the surface of the carbon fibers reduces the crosslinking density in the matrix due to the competing reactions between the epoxy resin and the newly deposited amino groups. This implies that to achieve reversibility properties provided by the D–A adducts comes at the cost to the overall mechanical performance of the composite. It is envisaged that a novel biobased epoxy resin systems must be developed which does not compete with the adduct reaction, to fully take advantage of this new reversible bonding system. This approach confirms that new biobased epoxy resins could be used to obtained fully recyclable systems. Besides, it opens a new research strategy in which matrix and fiber treatment are aligned toward the achievement of efficient crosslinking. This strategy brings eco-design and recyclability of composites a step closer.

AUTHOR CONTRIBUTIONS

The research has been distributed among all the co-authors. Prof. Jesus Cuartero has performed the LRI processes, as well as the mechanical characterization and the analysis of the results obtained. Ruth Garcia, Elisabeth Sanchez, and Mari Carme Royo carried out the amination of the CF and the contact angle characterization technique. Carlos Hornero has worked on the application of the different chemical structures for the formation of the D–A adduct on the surface of the fiber. Dr. Anne Beaucamp has been performing and analyzing the data obtained in the DMA tests carried out. Julio Vidal has been working through the research as a whole, as the main investigator and analyzing the data obtained from all the characterization techniques (collaborating all other authors in each of the characterizations) and specifically on the SEM and Raman characterization techniques. Finally, Dr. Pere Castell (Aitiip group leader), Prof. Maurice Collins, Dr. Lidia Garcia, and Dr. David Ponce have been closely supervising the research and analyzing the conclusions before taking the experiments to the next step. All authors have contributed in the writing and revision process of the manuscript.

CONFLICT OF INTEREST STATEMENT

The authors declare no conflict of interest.

DATA AVAILABILITY STATEMENT

The data that supports the findings of this study are available in the supplementary material of this article.

ORCID

Julio Vidal https://orcid.org/0000-0002-1094-0720
Carlos Hornero https://orcid.org/0009-0001-3934-6311
Ruth Garcia https://orcid.org/0000-0003-3844-8735
Jesus Cuartero https://orcid.org/0000-0002-6100-7412
Anne Beaucamp https://orcid.org/0000-0003-4746-7508
Maurice N. Collins https://orcid.org/0000-0003-2536-4508
Lidia Garcia https://orcid.org/0000-0003-1558-5526
David Ponce https://orcid.org/0000-0001-6044-3848
Mari Carme Royo https://orcid.org/0009-0005-3427-8355
Elisabeth Sanchez https://orcid.org/0009-0000-3969-7720
Pere Castell https://orcid.org/0000-0002-3611-9957

REFERENCES

1. Ferreira F, Pinheiro I, de Souza S, Mei L, Lona L. Polymer composites reinforced with natural fibers and nanocellulose in the automotive industry: A short review. *J Compos Sci.* 2019;3:51. doi:10.3390/jcs3020051

2. Ali HT, Akrami R, Fotouhi S, et al. Fiber reinforced polymer composites in bridge industry. *Structure.* 2021;30:774-785. doi:10.1016/j.istruc.2020.12.092

3. Office of Energy efficiency and renewable energy. Accessed March 29, 2023. https://www.energy.gov/eere/wind/articles/optimized-carbon-fiber-composites-wind-turbine-blade-design

4. Jagadeesh P, Puttegowda M, Oladijo OP. A comprehensive review on polymer composites in railway applications. *Polym Compos.* 2022;43:1238-1251. doi:10.1002/pc.26478

5. Muhammad A, Rahman MR, Baini R, Bakri MKB. *Advances in Sustainable Polymer Composites.* Elsevier; 2021:185-207.

6. He Y, Suliga A, Brinkmeyer A, Schenk M, Hamerton I. Atomic oxygen degradation mechanisms of epoxy composites for space applications. *Polym Degrad Stab.* 2019;166:108-120. doi:10.1016/j.polymdegradstab.2019.05.026

7. Bernatas R, Dagreou S, Despax-Ferreres A, Barasinski A. Recycling of fiber reinforced composites with a focus on thermoplastic composites. *Clean Eng Technol.* 2021;5:100272. doi:10.1016/j.clet.2021.100272

8. Yao S-S, Jin F-L, Rhee KY, Hui D, Park S-J. Recent advances in carbon-fiber-reinforced thermoplastic composites: A review. *Compos B: Eng.* 2018;142:241-250. doi:10.1016/j.compositesb.2017.12.007

9. Chukov DI, Stepashkin AA, Salimon AI, Kaloshkin SD. Highly filled elastomeric matrix composites: Structure and property evolution at low temperature carbonization. *Mater Des.* 2018;156:22-31. doi:10.1016/j.matdes.2018.06.034

10. Ouarhim W, Zari N, Bouhfid R, Qaiss AEK. *Fibre-Reinforced Composites and Hybrid Composites.* Elsevier; 2019:43-60. doi:10.1016/B978-0-08-102292-4.00003-5

11. Jagadeesh P, Mavinkere Rangappa S, Siengchin S, et al. Sustainable recycling technologies for thermoplastic polymers and their composites: A review of the state of the art. *Polym Compos.* 2022;43(9):5831. doi:10.1002/pc.27000

12. Abeykoon C, McMillan A, Nguyen BK. Energy efficiency in extrusion-related polymer processing: A review of state of the art and potential efficiency improvements. *Renew Sustain Energy Rev.* 2021;147:111219. doi:10.1016/j.rser.2021.111219

13. Zhang Y, Zhang L, Yang G, et al. Recent advances in recyclable thermosets and thermoset composites based on covalent adaptable networks. *J Mater Sci Technol.* 2021;92:75-87. doi:10.1016/j.jmst.2021.03.043

14. Hegde S, Satish Shenoy B, Chethan KN. Review on carbon fiber reinforced polymer (CFRP) and their mechanical performance. *Mater Today Proc.* 2019;19:658-662. doi:10.1016/j.matpr.2019.07.749

15. Muflikhun MA, Yokozeki T, Aoki T. The strain performance of thin CFRP-SPCC hybrid laminates for automobile structures. *Compos Struct.* 2019;220:11-18. doi:10.1016/j.compstruct.2019.03.094

16. Santhanakrishnan Balakrishnan V, Seidlitz H. Potential repair techniques for automotive composites: A review. *Compos B: Eng.* 2018;145:28-38. doi:10.1016/j.compositesb.2018.03.016

17. Sun Q, Zhou G, Meng Z, Jain M, Su X. An integrated computational materials engineering framework to analyze the failure behaviors of carbon fiber reinforced polymer composites for lightweight vehicle applications. *Compos Sci Technol.* 2021;202:108560. doi:10.1016/j.compscitech.2020.108560

18. Jin W, Zhang Y, Jiang L, Yang G, Chen J, Li P. Improvements in temperature uniformity in carbon fiber composites during microwave-curing processes via a recently developed microwave equipped with a three-dimensional motion system. *Compos B: Eng.* 2017;112:15-21. doi:10.1016/j.compositesb.2016.12.009

19. Chen K, Zhao G, Chen J, Zhu X, Guo S. Improvements in temperature uniformity in carbon fiber composites during microwave-curing processes via a recently developed microwave equipped with a three-dimensional motion system. *Materials.* 2023;16:705. doi:10.3390/ma16020705

20. Jin W, Zhang Y, Jiang L, Yang G, Chen J, Li P. A dynamic constitutive model and simulation of braided CFRP under high-speed tensile loading. *Materials.* 2022;15:6389. doi:10.3390/ma15186389

21. Bagheri S, Nejad M. Fully biobased composite made with epoxidized-lignin, reinforced with bamboo fibers. *Polym Compos.* 2023;1. doi:10.1002/pc.27366

22. Borodulin A, Kalinnikov A, Tereshkov A, Kharaev A. New polymeric binders for the production of composites. *Mater Today Proc.* 2019;11:139-143. doi:10.1016/j.matpr.2018.12.121

23. Pizzi A, Papadopoulos AN, Policardi F. Wood composites and their polymer binders. *Polymers (Basel).* 2020;12:1115. doi:10.3390/polym12051115

24. Agustiany EA, Rasyidur Ridho M, Rahmi DNM, et al. Recent developments in lignin modification and its application in lignin-based green composites: A review. *Polym Compos.* 2022;43(8):4848. doi:10.1002/pc.26824

25. Kanthraju S, Vinodhini J, Bhowmik GMS. An investigation to enhance the mechanical property of high-performance thermoplastic composite through different plasma treatment. *Polym Compos.* 2023;44(1):178. doi:10.1002/pc.27037

26. Nelyub VA, Borodulin AS, Kobets LP, Malysheva GV. A study of structure formation in a binder depending on the surface microrelief of carbon fiber. *Polym Sci Ser D.* 2016;9:286-289. doi:10.1134/S1995421216030187

27. Zheng Y, Wang X, Wu G. Chemical modification of carbon fiber with diethylenetriaminepentaacetic acid/halloysite nanotube as a multifunctional interfacial reinforcement for silicone resin composites. *Polym Adv Technol.* 2020;31:527-535. doi:10.1002/pat.4793

28. Zanjani JSM, Baran I. Co-bonded hybrid thermoplastic-thermoset composite interphase: Process-microstructure-property correlation. *Materials.* 2021;14:291. doi:10.3390/ma14020291

29. Nasreen A, Bangash MK, Shaker K, Nawab Y. Effect of surface treatment on the performance of composite-composite and composite-metal adhesive joints. *Polym Compos.* 2022;43(9):6320. doi:10.1002/pc.26940

30. Khalil YF. Eco-efficient lightweight carbon-fiber reinforced polymer for environmentally greener commercial aviation industry. *Sustain Prod Consum.* 2017;12:16-26. doi:10.1016/j.spc.2017.05.004

31. Culebras M, Beaucamp A, Wang Y, Clauss M, Frank E, Collins MN. Biobased structurally compatible polymer blends

based on lignin and thermoplastic elastomer polyurethane as carbon fiber precursors. *ACS Sustain Chem Eng.* 2018;6:8816-8825. doi:10.1021/acssuschemeng.8b01170

32. Steudle LM, Frank E, Ota A, et al. Hydrothermal carbon as reactive fillers to produce sustainable biocomposites with aromatic bio-based epoxy resins. *Macromol Mater Eng.* 2017;302:1600441. doi:10.1002/mame.201600441

33. Bejenari I, Dinu R, Montes S, Volf I, Mija A. Hydrothermal carbon as reactive fillers to produce sustainable biocomposites with aromatic bio-based epoxy resins. *Polymers (Basel).* 2021;13:240. doi:10.3390/polym13020240

34. Ginder RS, Ozcan S. Recycling of commercial e-glass reinforced thermoset composites via two temperature step pyrolysis to improve recovered fiber tensile strength and failure strain. *Dent Rec.* 2019;4:24. doi:10.3390/recycling4020024

35. Prinçaud M, Aymonier C, Loppinet-Serani A, Perry N, Sonnemann G. Environmental feasibility of the recycling of carbon fibers from cfrps by solvolysis using supercritical water. *ACS Sustain Chem Eng.* 2014;2:1498-1502. doi:10.1021/sc500174m

36. Bin Rusayyis MA, Torkelson JM. Reprocessable covalent adaptable networks with excellent elevated-temperature creep resistance: Facilitation by dynamic, dissociative bis(hindered amino) disulfide bonds. *Polym Chem.* 2021;12:2760-2771. doi:10.1039/D1PY00187F

37. Di Mauro C, Malburet S, Genua A, Graillot A, Mija A. Sustainable series of new epoxidized vegetable oil-based thermosets with chemical recycling properties. *Biomacromolecules.* 2020;21:3923-3935. doi:10.1021/acs.biomac.0c01059

38. Di Mauro C, Genua A, Mija A. Bioinspired fracture toughness enhancement of a fully bio-based epoxy resin. *Ind Crops Prod.* 2022;185:115116. doi:10.1016/j.indcrop.2022.115116

39. Chakma P, Morley CN, Sparks JL, Konkolewicz D. Exploring how vitrimer-like properties can be achieved from dissociative exchange in anilinium salts. *Macromolecules.* 2020;53:1233-1244. doi:10.1021/acs.macromol.0c00120

40. Krishnakumar B, Sanka RVSP, Binder WH, Parthasarthy V, Rana S, Karak N. Vitrimers: Associative dynamic covalent adaptive networks in thermoset polymers. *Chem Eng J.* 2020;385:123820. doi:10.1016/j.cej.2019.123820

41. Xu X, Ma S, Wang S, et al. Fast-reprocessing, postadjustable, self-healing covalent adaptable networks with schiff base and diels–alder adduct. *Macromol Rapid Commun.* 2022;43:2100777. doi:10.1002/marc.202100777

42. Quiles-Díaz S, Seyler H, Ellis GJ, et al. Designing new sustainable polyurethane adhesives: Influence of the nature and content of Diels-Alder adducts on their Thermoreversible behavior. *Polymers (Basel).* 2022;14:3402. doi:10.3390/polym14163402

43. Peterson AM, Jensen RE, Palmese GR. Thermoreversible and remendable glass–polymer interface for fiber-reinforced composites. *Compos Sci Technol.* 2011;71(5):586-592. doi:10.1016/j.compscitech.2010.11.022

44. Longana ML, Tapper RJ, Blok LG, Hamerton I. *Fiber Reinforced Composites.* Elsevier; 2021:561-595.

45. Zhang W, Duchet J, Gérard JF. Self-healable interfaces based on thermo-reversible Diels–Alder reactions in carbon fiber reinforced composites. *J Colloid Interface Sci.* 2014;430:61-68. doi:10.1016/j.jcis.2014.05.007

46. Lee AY, Yang K, Anh ND, et al. Raman study of D* band in graphene oxide and its correlation with reduction. *Appl Surf Sci.* 2021;536:147990. doi:10.1016/j.apsusc.2020.147990

47. Li G, Lee-Sullivan P, Thring RW. Determination of activation energy for glass transition of an epoxy adhesive using dynamic mechanical analysis. *J Thermal Anal Calorim.* 2000;60:377-390. doi:10.1023/A:1010120921582

48. Jacob M, Francis B, Thomas S, Varughese KT. Dynamical mechanical analysis of sisal/oil palm hybrid fiber-reinforced natural rubber composites. *Polym Compos.* 2006;27(6):671-680. doi:10.1002/pc.20250

49. Karbhari VM, Wang Q. Multi-frequency dynamic mechanical thermal analysis of moisture uptake in E-glass/vinylester composites. *Compos Part B: Eng.* 2004;35(4):299-304. doi:10.1016/j.compositesb.2004.01.003

SUPPORTING INFORMATION

Additional supporting information can be found online in the Supporting Information section at the end of this article.

How to cite this article: Vidal J, Hornero C, Garcia R, et al. Use of covalent dynamic networks as binders on epoxy-based carbon fiber composites: Effect on properties, processing, and recyclability. *Polym Compos.* 2023;1-13. doi:10.1002/pc.27636